

A spatially explicit modeling analysis of adaptive variation in temperate tree phenology

Liang Liang

Department of Geography, University of Kentucky, 817 Patterson Office Tower, Lexington, KY, 40506-0027, United States

ARTICLE INFO

Keywords:
 Bud break
 Leaf senescence
 Spring phenology
 Autumn phenology
 Climate adaptation
 Phenological models

ABSTRACT

The geographic applicability of most phenological models is limited because of a lack in accounting for plant genotypic variation over space. This limitation may be partly addressed by quantifying plant adaptation patterns as revealed by common garden/provenance trial research. This study delineated adaptive patterns of a widely distributed tree species in North America—white ash (*Fraxinus americana*) using multi-year common garden observations of leaf out and leaf senescence phenology. Geographically varied phenology-climate (i.e., pheno-climatic) relationships of tree provenances were investigated both with the aid of interannual temperature variations and using process-based models. Interannual weather fluctuations likely led to varied gradients of spring phenological timing by tree origin latitude as influenced by interactions of chilling and forcing, while the latitudinal gradient of autumn phenology consistently followed a photoperiod-driven pattern. Fitted models revealed latitudinal gradients of chilling requirement (for dormancy release), forcing requirement (for bud break), and critical day length requirement (for leaf senescence) for the tree provenances. When these genotype-specific pheno-climatic relationships were accounted for in spring models, predictions closely matched the latitudinal gradient of USA-National Phenology Network (NPN) observations. On the other hand, average (non-spatial) model predictions of bud break tended to be biased in the species' northern and southern ranges. This finding shows that introducing genotypic differences to phenological models is necessary for accurate prediction of temperate tree phenology over broad geographic regions.

1. Introduction

Phenology studies the timing and interrelation of recurring biological events that are driven by both biotic and abiotic forces in the seasonal environment (Lieth, 1974). Temperate plants, in particular, are adapted to respective seasonal temperature and photoperiod regimes to regulate the timing of annual growth and dormancy cycles at varied geographic locations (Basler and Körner, 2014; Chuine et al., 2010; Cooke et al., 2012). It is well recognized that changes in phenological timing directly affect ecological processes such as primary production (Richardson et al., 2010; Wu et al., 2013; Xia et al., 2015), biogeochemical cycling and exchange (Balzalero et al., 2016; Churkina et al., 2005; Melaas et al., 2013), trophic interactions and synchrony (Donoso et al., 2016; Fogelström et al., 2017; Rafferty et al., 2015), and species distribution and range shift (Chuine, 2010; Chuine and Beaubien, 2001; Morin and Thuiller, 2009). Moreover, the importance of plant phenology as an indicator of biosphere-climate interactions and changes has led to an increased effort in data collection and method development in support of phenological predictions over broad geographic regions (Ault et al., 2015; Crimmins et al., 2017; Hufkens et al.,

2018). However, the use of phenology as an effective ecological forecasting tool is still hindered by a lack of accounting for the underlying genotypic variability of plants in phenological models.

As this task is often difficult, most plant phenology models either treat observations at various locations as being genetically distinct from each other or assume a uniform plant response to different climate conditions. On the one hand, models based on discrete datasets are applicable only to specific plant populations of selected species, lacking expendability to additional populations at different locations (Chuine et al., 2013; Chuine and Régnière, 2017). On the other hand, continental-scale and wall-to-wall phenological prediction is currently made possible only by cloned-plant-based models, which assume a constant plant-climate relationship over space (Schwartz et al., 2006, 2013). Both approaches assume that genotypic variations may be either random or negligible because there are no specific geographic patterns that can be followed to quantify them. Despite that such simplifications are necessary to allow models to be developed over constrained datasets, they limit the ability of these models to make geographically realistic predictions.

If the genotypic variability among plant populations were spatially

E-mail address: liang.liang@uky.edu.

<https://doi.org/10.1016/j.agrformet.2018.12.004>

Received 29 August 2018; Received in revised form 1 December 2018; Accepted 6 December 2018

Available online 14 December 2018

0168-1923/© 2018 Elsevier B.V. All rights reserved.

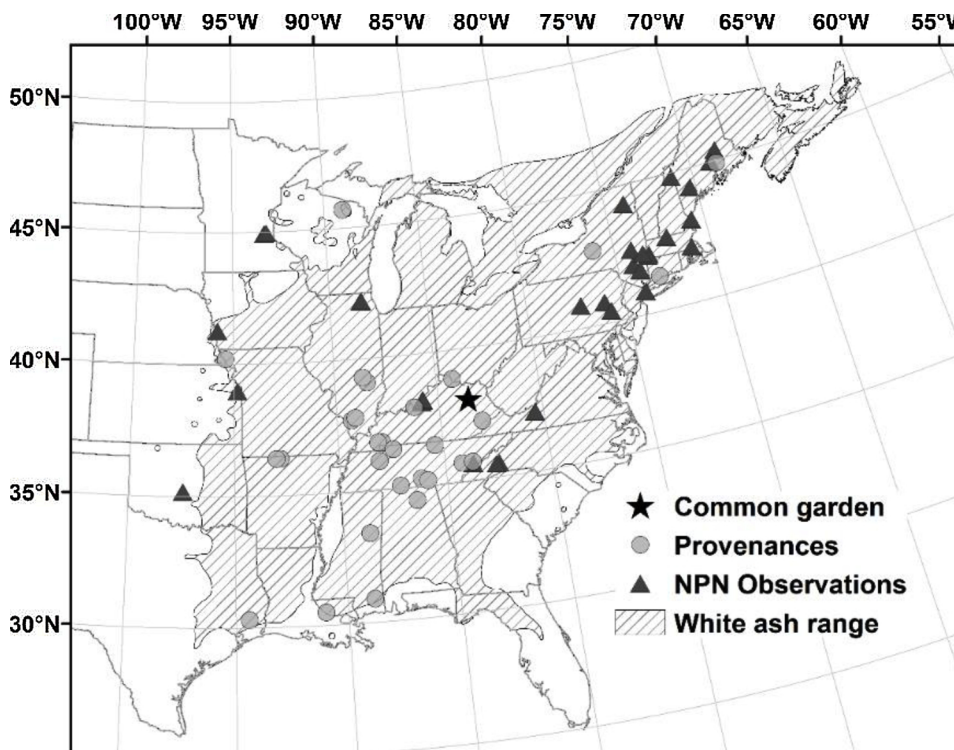


Fig. 1. Study area map showing 1) the distribution range of white ash (*Fraxinus americana*; Little, 1971), 2) the common garden location in Kentucky, U.S., 3) the source locations of the provenances represented in the common garden, and 4) USA-National Phenology Network (NPN) spring phenology observations (2009–2016) of the same species.

random, we would be unable to make interpolation or extrapolation at unobserved locations. Fortunately, since plant phenological traits are fundamentally adapted to long-term climatic differences across space (Lechowicz, 1984; Preite et al., 2015), the spatial predictability of genotypic difference to a large extent hinges upon the identifiability of specific climate adaptation patterns. Indeed, the adaptation-based genetic difference in plant phenology has long been recognized (Flint, 1974; Hänninen, 2016; Nienstaedt, 1974), albeit the use of it in spatial modeling is rare. Early research investigated the impact of genetic variations of five European tree species on phenological model predictions (Chuine et al., 2000). In recent years, progress has been made to describe the clinal variability of European beech (*Fagus sylvatica* L.) bud break phenology in process-based models (Kramer et al., 2015, 2017). More research along this line, especially on additional species that are widely distributed, is needed to further our ability to incorporate adaptive variation in spatially-explicit phenological models.

Knowledge about adaptive variation in plant phenology has been mostly gained through common garden/provenance trial studies (Mátyás, 1996; Vitasse et al., 2009; Zohner and Renner, 2014). Although any observed phenology only directly reflects plant phenotypes, which are a result of genotype × environment interaction, growth variations among tree provenances in common gardens (in which the environment is held constant) have long been used to quantify plant genotypic variability in forest genetics research (Wright, 1944, 1976). Liang (2016) reviewed relevant studies and summarized several common adaptive patterns for spring and autumn phenology of temperate tree species. These adaptive patterns are characterized by geographically-varied climatic requirements of tree provenances for regulating the start and end of growing season as a strategy to optimize the tradeoff between survival (in relation to frost avoidance) and growth in temperate and boreal environments (Hänninen, 2016; Kramer et al., 2017). In spring, provenances of a species that are adapted to colder climates (e.g., from more northern/high-latitude locations) likely require more chilling (for endodormancy release; Rohde and Bhalerao, 2007) but less forcing (i.e., heat sum) for triggering bud break than warmer-climate-adapted provenances (Kriebel, 1957; Kriebel and Wang, 1962). In autumn, leaf senescence is predominantly photoperiod

driven, with provenances from higher latitudes requiring longer critical day length (or shorter night length) than those from lower latitudes (Rohde and Bhalerao, 2007; Vaartaja, 1959). These different environmental requirements with the definable spatial/clinal patterns with respect to provenance source locations provide a basis for predicting genotype-based phenological variability among plant populations. Certainly, such adaptive patterns must vary in character and scale by species and regions, and therefore should be examined specifically for each case before being used in phenological models.

In this study, I investigated common garden phenology of white ash (*Fraxinus americana*) to characterize its adaptive patterns in support of spatially-explicit models. Previous common garden observations suggested strong clinal variations in the species' phenology but there were not enough details available to allow for quantifying its adaptive patterns in relation to specific climatic requirements (Bey et al., 1976; Clausen, 1980; Marchin, 2006; Wendel, 1984). A foregoing work has initially quantified the climate adaptation variability of white ash phenology using concurrent common garden observation and meteorological measurement (Liang, 2015). In this study, I further characterized the species' adaptive patterns using additional observations and process-based models. The overarching goal of the research is to develop and test methods for incorporating adaptation-based genotypic variations into phenological models of temperate tree species.

2. Data and methods

2.1. Field observations and data

Field data used in this study included multi-year observations from a common garden and spatially distributed observations from the USA National Phenology Network (NPN). The modeling was based on the common garden data, and the predictions were tested using the NPN data (for spring only). The white ash common garden experiment is located in the Daniel Boone National Forest, Rowan County, Kentucky, United States (Fig. 1). White ash is native to eastern North America and is widely distributed over a broad climatic range (Cf. Fig. 1; Little, 1971). The plantation was established in 1976 in the middle range as

Table 1

Summary information of white ash (*Fraxinus americana*) provenances in the common garden in Kentucky, U.S., covering their geographic locations and live tree counts (#Trees) as of spring 2013 and spring 2017, at the beginning and end of field observations.

Provenance	Latitude	Longitude	Elevation (ft)	State	County	#Trees (2013)	#Trees (2017)
1	45.7	-89.0	1675	Wisconsin	Forest	1	0
2	44.9	-68.6	100	Maine	Penobscot	0	0
3	42.8	-76.1	1600	New York	Onondaga	2	0
4	41.3	-73.0	300	Connecticut	New Haven	8	7
5	40.2	-95.4	975	Nebraska	Richardson	7	2
6	39.3	-88.6	630	Illinois	Shelby	10	1
7	39.1	-88.4	600	Illinois	Effingham	19	7
8	38.9	-84.2	800	Ohio	Warren	13	4
9	38.0	-86.2	650	Indiana	Harrison	11	5
10	37.8	-89.1	400	Illinois	Williamson	36	19
11	37.7	-89.3	450	Illinois	Jackson	12	5
12	37.2	-83.0	1250	Kentucky	Perry	19	7
13	36.8	-87.9	510	Kentucky	Trigg	19	13
14	36.5	-85.4	1180	Tennessee	Overton	44	27
15	36.5	-87.4	650	Tennessee	Robertson	25	9
16	36.4	-92.8	900	Arkansas	Marion	18	12
17	36.4	-93.0	900	Arkansas	Boone	13	5
18	35.7	-84.2	980	Tennessee	Monroe	16	11
19	35.7	-83.7	1350	Tennessee	Blount	15	13
20	35.3	-86.2	1070	Tennessee	Coffee	13	12
21	35.2	-85.9	1115	Tennessee	Franklin	13	6
22	35.1	-87.2	900	Tennessee	Lawrence	14	9
23	34.5	-86.5	1000	Alabama	Madison	23	13
24	33.4	-88.8	380	Mississippi	Oktibbeha	28	6
25	30.9	-88.8	250	Mississippi	George	9	1
26	30.5	-91.0	100	Louisiana	E. Bat. Rou.	9	0
27	30.3	-94.4	100	Texas	Hardin	5	0

part of a range-wide provenance test of the species (Clausen, 1980). The site configuration and layout has been described in detail in Liang (2015). In brief, the plantation originally included 1025 trees from 27 white ash provenances. Over the years, the number of trees has declined, with 402 live trees from 26 provenances remaining in 2013, and only 194 trees from 22 provenances in 2017 (Table 1). The tree decline was exacerbated by an emerald ash borer (*Agrilus planipennis*) infestation since 2015. Each season of field observation covered all live trees at the time, leading to varied numbers of observation across years. For model fitting, provenances that were still represented by at least one live tree in 2017 (Cf. Table 1; numbered 4 through 25) were included given their larger sample sizes and a longer data duration.

Both spring and autumn phenological data were collected from the common garden. The author (as the only observer) traveled weekly to the study site during each season and observed the phenological status of all live trees using binoculars (for more details please see Liang, 2015). The field observation continued from spring 2013 to spring 2017 and ceased when significant loss of canopy cover (caused by the before-mentioned emerald ash borer infestation) occurred in summer 2017. This produced a five-year-long dataset covering five spring seasons (2013–2017) and four autumn seasons (2013–2016) in total. The visual observations followed a protocol describing continuous processes of leaf out and leaf senescence (Liang et al., 2011; Yu et al., 2016). The protocol scored spring and autumn phenophases that include buds open (leaves visible, 300), leaves out (not fully unfolded, 400), leaves fully unfolded (500), leaf coloration (800), and leaf fall (900). A percentage range estimate relative to the degree at which a canopy had reached a certain phenophase was added upon each score reading (e.g., 390 = “buds open > 90%”).

Given that most phenological data and models target phenological events, critical transition dates of spring and autumn phenophases were extracted from the phenological score time series. Specifically, dates of Initial Bud Break (IBB, buds open < 10%) and Full Bud Break (FBB, buds open > 90%) were determined. In case IBB or FBB for a specific tree did not occur on an observation day, a date was estimated for that tree using linear interpolation of the two adjacent scores (Liang, 2015).

The IBB phenophase was focused on and used for model development given that it marks the beginning of leaf out and corresponds with the NPN's phenometric—Breaking Leaf Buds (BLB). Despite that there was no corresponding NPN phenometric for FBB, this phenophase was included in initial data analysis only for additional descriptions of spring phenology variability. Dates of two autumn phenological events: Full Leaf Coloration (FLC, leaf coloration > 90%) and Full Leaf Fall (FLF, leaf fall > 90%) were extracted in a similar manner. The FLC phenophase was focused on for model development with FLF included in initial analyses for a more complete characterization of autumn phenology variation. White ash phenometric data from 2009 to 2016 were downloaded from the NPN website (USA National Phenology Network, 2017). There was a total of 211 BLB observations from 50 different locations (Fig. 1). The number of observations increased each year since the NPN was established in 2009. Autumn phenometric observations for white ash were also available from the NPN dataset, but were not used because they were small in sample size (< = 35) and were from only a few locations.

Concurrent hourly temperature measurement was taken at the plantation using two automatic iButtons (Embedded Data Systems, Lawrenceburg, Kentucky). Additional hourly temperature data from a nearby (~ 12 km) weather station at Morehead were acquired from the Kentucky Mesonet to fill in data gaps during the following time periods: 1) Sep. 2012 to Jan. 2013, prior to the deployment of iButtons; and 2) Oct. 2015 to Apr. 2016, when the first two iButtons expired before they could be replaced. A 0.77 °C difference between the weather station and on-site measurements during an overlapped period was found. Hence, weather station temperature values were calibrated using a linear relationship established with all temporally-overlapped on-site data. These hourly data were then averaged to daily mean temperatures for modeling and analysis. Corresponding to the NPN BLB observations, daily maximum and minimum temperatures at all data locations for all available years were extracted from the gridded Daymet product (V3, <https://daymet.ornl.gov/>). The extracted Daymet daily maximum and minimum temperatures were then averaged to produce daily mean temperatures for subsequent modeling and analysis.

2.2. Data analysis and modeling

Initial data analyses were conducted prior to model fitting to reveal both general phenological variations and specific variations caused by different tree origins. First, interannual variations of phenological dates in relation to seasonal temperature change were explored using box-plots and side-by-side comparisons irrespective of provenances. Variation of mean leaf bud break dates was compared to the fluctuation of spring mean temperature, and variation of mean leaf senescence dates was compared to the fluctuation of autumn mean temperature. Photoperiod was not considered here given that its cycle at a fixed location (i.e., in the common garden) does not vary across years but remains static. The respective seasonal periods were divided using the 24 solar terms according to the traditional Chinese calendar (Aslaksen, 2010). This system expands upon the four seasonal markers (i.e., equinoxes and solstices) to include 20 additional equally-spaced positions/dates along the Earth's orbit around the Sun. These dates were historically used in China as part of a general farmer's almanac and are both related and characterized by seasonal and biometeorological changes. Based on this system, winter was marked as the time period from Nov. 7 to Feb. 3, followed by spring that lasts until May 5; and autumn from Aug. 8 to Nov. 6. These seasonal divisions are potentially more useful for calculating seasonal temperatures that impact phenology, because for instance, temperate trees likely have begun responding to warm temperatures before the start dates of astronomical spring and meteorological spring (Mar. 21 and Mar. 1, respectively), but after the coldest month (i.e., Jan. for most Northern Hemisphere land locations).

Further, gradients of phenological dates by tree origin latitude were compared to seasonal mean temperatures (following the same seasonal divisions as described previously) at the common garden. Given that the white ash common garden is located in the central range of the species (Fig. 1), varied winter and spring temperature regimes during respective years of observation may trigger gradients of opposite directions (Liang, 2015, 2016). Specifically, in the Northern Hemisphere, bud break may occur earlier with southern provenances and agrees with what is observed *in situ* at the provenance source locations, hence referred to as a cogradient pattern; or the gradient may be contrary to what is observed *in situ*, i.e., with bud break happening earlier with northern provenances, hence a countergradient pattern. This is based on the assumption that, like many other temperature species, northern provenances of white ash have higher chilling requirements and lower forcing requirements than southern provenances (see review by Liang, 2016). Therefore, a cogradient pattern may occur when the fulfillment of the chilling requirements of northern provenances is retarded in a common garden; or a countergradient may occur when the differential forcing requirements determine the bud break sequence after the chilling requirements of most provenances are satisfied. Indefinite patterns could also occur when neither environmental factor is dominant. For leaf senescence, a consistent cogradient pattern (i.e., northern provenances change leaf color earlier in response to longer critical day length) for white ash is expected as for many other tree species (Bey et al., 1976; Clausen et al., 1981; Way, 2011).

Finally, these differential environmental requirements of phenological events were investigated using process-based models. The dates of Initial Bud Break (IBB) and Full Leaf Coloration (FLC) were predicted using functions of antecedent temperature conditions, and photoperiod (for FLC only). Model selection and fitting were performed using the Phenology Modelling Platform (PMP; Chuine et al., 2013), and additional analyses were done using R (R Core Team, 2018). The additional data analyses included 1) preprocessing temperature and phenology data; 2) statistical analyses; and 3) graphic presentation of results. Given a lack of ecophysiological information for comprehensively parameterizing the models, an intermediate approach, which lies between a full experiment-supported approach and one that relies altogether on statistical fitting (Hänninen, 2016), was taken to fit the

provenance-specific climatic requirements on the basis of *a priori* information. Both literature of previous modeling work and an iterative testing process were engaged to determine the fixed parameters that optimize the differentiation of climatic requirements among provenances. In particular, to distinguish the respective effects of chilling and forcing, a two-phase sequential model was adopted for IBB as follows,

$$S_c = \sum_{t_0}^{t_1} R_c(T) = C^* \quad (1)$$

where S_c is the state of chilling, which is a function of the time integral of the rate of chilling (R_c), approximated with a summation of the responses to cooler daily mean temperatures (T). The accumulation of chilling starts from an initial date (t_0) in autumn until the critical chilling requirement (C^*) is met (t_1 , i.e., rest completion). Sept. 1 was arbitrarily chosen for t_0 in reference to previous modeling practices (Chuine, 2000; Hänninen and Kramer, 2007).

$$S_f = \sum_{t_1}^{t_2} R_f(T) = F^* \quad (2)$$

where S_f is the state of forcing, which is calculated as a time integral of the rate of forcing (R_f), approximated with a summation of the responses to warmer daily mean temperatures (T). The forcing accumulation starts after the rest completion (t_1) and continues until the critical forcing requirement (F^*) is met (t_2), i.e., when predicted leaf bud break occurs.

The response function for the rate of chilling (R_c) followed the smoothed Utah method (Bonhomme et al., 2010; Richardson et al., 1974). This approach assumes that the chilling effect is most effective at an optimal temperature, and the chilling effectiveness decreases when the temperature is lower or higher than the optimum, gradually reaching zero towards lower temperatures and may become negative under warmer temperatures. In this study, the smoothed Utah function was parameterized with temperature thresholds used in the original step-wise Utah model (Richardson et al., 1974). The chilling response curve was constrained with 6 °C as the optimal temperature for full cold efficiency (1), which quickly decreased to zero below freezing and became negative beyond 15 °C (and gradually down to -1). The readers may refer to the documentation of PMP (Chuine et al., 2013) for a more detailed description of the function. After chilling fulfillment and rest completion (t_1), the rate of forcing was calculated using growing degree days with a base temperature of 5 °C. Cold storage experiments showed that white ash seedlings both received effective chilling and were kept in the state of quiescence at this temperature (Webb, 1976, 1977). The same base temperature of 5 °C was also used in previous modeling practice (Hänninen, 2016).

Fall phenology is far less studied than spring phenology; and leaf senescence model development is still at its incipient stage (Chuine et al., 2013; Gallinat et al., 2015). Among a few available algorithms, one driven by both photoperiod and cool temperatures (Delpierre et al., 2009) was adopted for FLC modeling. The inclusion of a critical photoperiod parameter in this model allowed differentiating the different photoperiod requirements of provenances. The function can be expressed as follows,

$$S_s = \sum_{t_0}^{t_1} R_s(T, P) = \sum_{t_0}^{t_1} \begin{cases} 0 & \text{if } (P > P_b) \text{ or } (T > T_b) \\ (T_b - T)^{\alpha*} \left(\frac{P}{P_b}\right)^{\beta} & \text{if } (P \leq P_b) \text{ and } (T \leq T_b) \end{cases} = S^* \quad (3)$$

where S_s is the state of senescence, which is a time integral of the rate of senescence (R_s) after an arbitrary initial date (t_0). The rate of senescence responds to both cooling temperatures (T) and declining photoperiod (P). The model assumes that leaf senescence process is driven by relatively cool temperatures (below a base T_b) and/or shorter day lengths (below a critical base P_b). The relative importance of temperature and photoperiod is accounted for by two additional parameters (α and β).

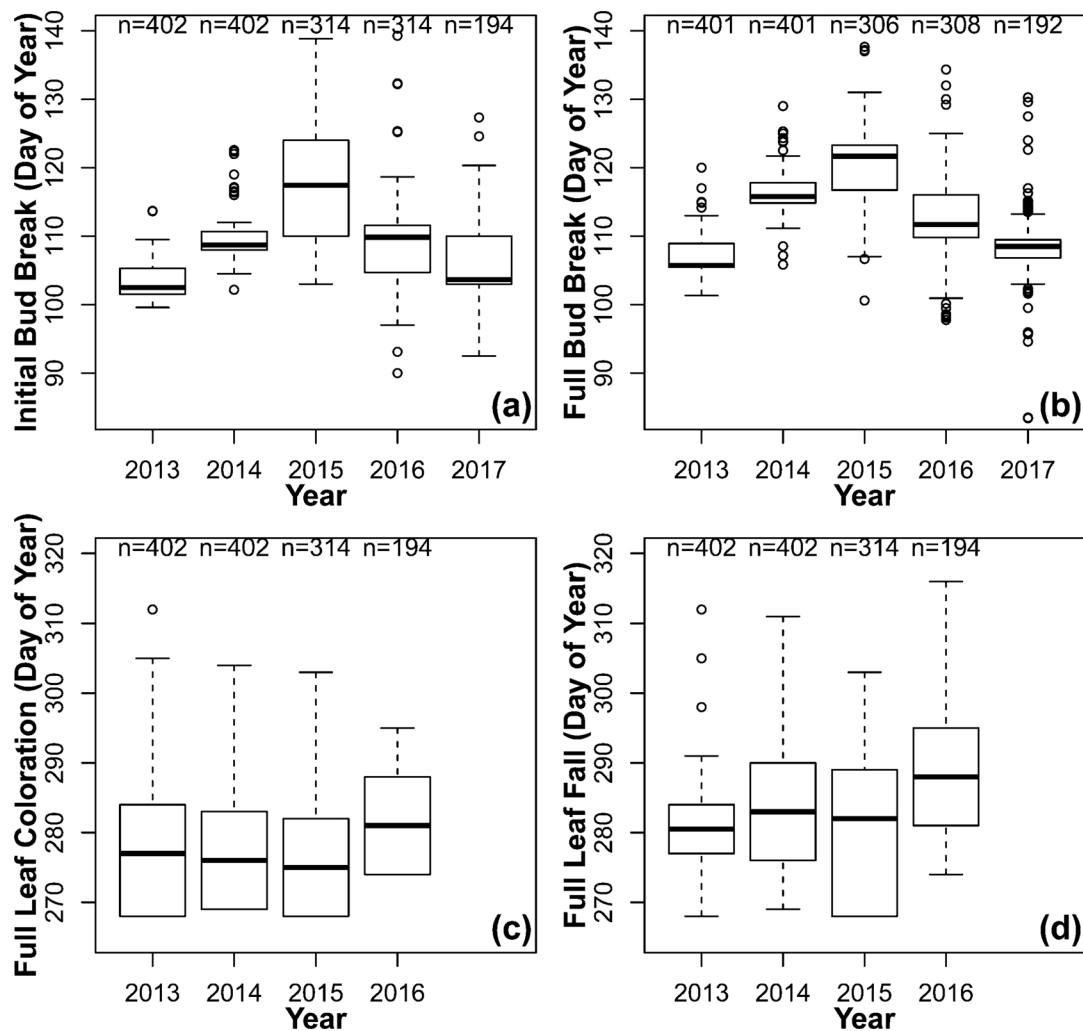


Fig. 2. Boxplots of white ash (*Fraxinus americana*) common garden phenological observations of (a) Initial Bud Break, (b) Full Bud Break, (c) Full Leaf Coloration, and (d) Full Leaf Fall dates (in Day of Year) for all available trees in respective years.

The leaf senescence event (i.e., FLC) occurs at t_1 as the state of senescence reaches a critical value (S^*). In the modeling of FLC, t_0 was set as Aug. 8th, the beginning of autumn season according to the seasonal division by solar terms. Previous studies empirically fitted 20 °C (Richardson et al., 2006; Yu et al., 2016) or 25–28.5 °C (depending on species; Delpierre et al., 2009) as thresholds for autumn cooling temperature calculation. In this study, T_b was set to 15 °C given that it optimized the models in terms of photoperiod requirement differentiation in comparison to several other temperature thresholds that were tested (i.e., 10 °C, 20 °C, 25 °C, and 30 °C). Due to a lack of additional *a priori* information, other parameters were fitted.

2.3. Simulation and model testing

The parameterized models were fitted to all available data from each provenance, respectively. Model performance was internally evaluated using root mean square error (RMSE) defined as follows,

$$RMSE = \sqrt{\frac{\sum_{i=1}^n (O_i - P_i)^2}{n}} \quad (4)$$

where O_i represents observed dates for a phenophase; P_i represents predicted dates; and n is the number of observations. For each

phenophase/provenance, 20 replicate runs were performed and the model with the lowest RMSE was chosen albeit that the differences among results from different runs were very small. Then the geographic relationship between fitted climate requirement parameters of the models and tree origin latitudes was investigated using linear regression.

The spring phenology model predictions were further tested using NPN observations. The BLB observations from the NPN were filtered by removing any dates that were beyond the day of year 180, leaving 193 (out of 211) records. First, based on the linear relationships established for differential chilling and forcing requirements (C^* and F^*) of IBB relative to latitude, respective C^* and F^* parameter values applicable to the locations (i.e., latitudes) of NPN data were determined. Then models based on these genotype-specific parameters (i.e., spatially-explicit models or simply a “spatial model”) were used to predict IBB dates for all locations/years with NPN observations. The same sequential model was also directly fitted to all NPN BLB data irrespective of their geographic locations (hence an “average model”). The predictions from the spatial model and the average model were compared to NPN observations, respectively. Given a lack of normality in residuals of analysis of covariance, a bootstrapping method (Davison and Hinkley, 1997) was used to compare the predictions and observations in terms of their difference and similarity along latitudinal gradient.

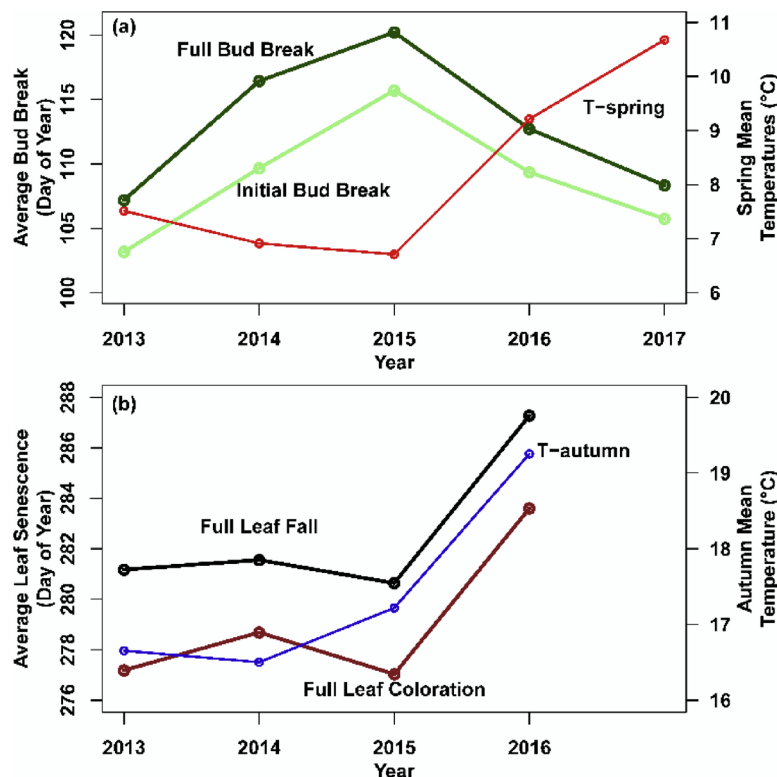


Fig. 3. Side-by-side comparison of (a) average Initial Bud Break and Full Bud Break dates (in Day of Year) with spring mean temperatures, and (b) average Full Leaf Coloration and Full Leaf Fall dates with autumn mean temperatures at the common garden across years.

This non-parametric approach established linear models based on resampling (with replacement) of the data 10,000 times from the observed and predicted bud break dates, respectively. Confidence intervals of the model parameters (intercept and slope) were estimated at a preset significance level of 0.05.

Given the lack of autumn phenology data from the NPN (as noted previously), FLC models were further tested externally using leave-one-out cross-validation (Chuine et al., 2016; Chuine and Régnière, 2017). Accordingly, the root mean square error for prediction (*RMSEP*) was computed. The *RMSEP* follows the same equation as *RMSE* (Eq. 4) except that the pairs of observed and predicted dates were the ones left out from model fitting runs.

3. Results

3.1. Overall interannual variations

Dates of Initial Bud Break (IBB) and Full Bud Break (FBB) both varied markedly across years with respect to medians and interquartile ranges (Fig. 2a and b). During the five years of observation, the median dates of IBB varied between the day of year 103 to 117, and the interquartile range fluctuated between 4 and 13 days. The median dates of FBB varied between 106 and 122, and its interquartile range fluctuated between 3 and 7 days. Dates of Full Leaf Coloration (FLC) and Full Leaf Fall (FLF) had smaller interannual variations than those of spring phenological events (Fig. 2c and d). The median dates of FLC and FLF only varied from 275 to 281 and 281 to 288, respectively. The interquartile range varied from 14 to 16 days for FLC, and 7 to 21 days for FLF. Hence, compared to dates of spring phenology, dates of autumn phenology were more spread out among individuals each year, but less

variable across years. In addition, FLF was more variable across years than FLC as indicated by its larger interquartile range variation (14 days vs. 2 days).

Interannual variations in the average dates of the phenological events generally mirrored the fluctuation of seasonal mean temperatures (Fig. 3). Earlier bud break occurred during years with warmer spring temperatures (Fig. 3a), while later autumn phenology concurred with warmer autumn mean temperatures (Fig. 3b). The autumn temperature effect on leaf senescence timing was not clear from 2013 through 2015 (with small temperature changes) but was highlighted in 2016.

3.2. Interannual variation with respect to latitudinal gradients

The gradients of spring phenological timing relative to tree origin latitude varied in both quantity and direction across years (Fig. 4, Table 2). IBB showed significant (*p*-value < 0.01) cogradient patterns (i.e., positive slopes, buds broke earlier in southern provenances) in 2013, 2016, and 2017, and a significant countergradient pattern (i.e., negative slopes, buds broke earlier in northern provenances) in 2015. FBB showed significant (*p*-value < 0.01) cogradient patterns in 2013 and 2016, and a significant countergradient pattern in 2014. The gradients of spring phenophases are mostly weak despite that they are statistically significant. Autumn phenological events (FLC and FLF), on the other hand, consistently showed significant (*p*-value < 0.01) and stronger cogradient patterns (i.e., negative slopes, northern provenances were earlier) for all occasions (Fig. 5, Table 2). Please note that a negative slope for autumn phenology is cogradient (opposite to that of spring phenology) because leaf senescence occurs earlier *in situ* at higher latitudes.

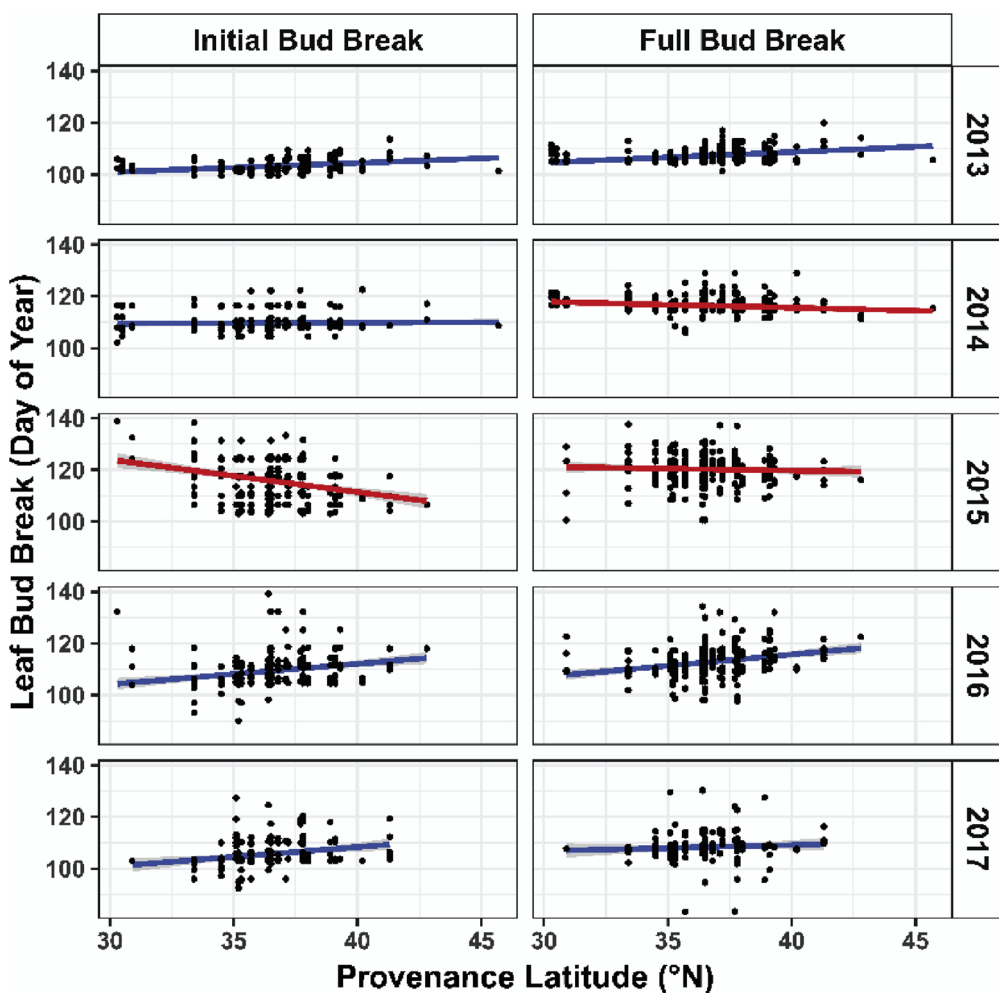


Fig. 4. Annual gradients of Initial Bud Break and Full Bud Break dates (in Day of Year) relative to provenance latitude (Cf. Table 2). All positive slopes indicate a cogradient pattern (marked in blue), while the negative slopes indicate a countergradient pattern (marked in red) (For interpretation of the references to colour in this figure legend, the reader is referred to the web version of this article).

Table 2

Linear models of the annual gradients (Cf. Fig. 4 and Fig. 5) of the spring and autumn phenophase dates (Y) against provenance latitude (X). An asterisk indicates a significant relationship.

Year	Phenophase	Linear Equation	R ²	p-value	Gradient Type
2013	Initial Bud Break	$Y = 0.36X + 90.19$	0.12	< 0.01*	Cogradient
2014	Initial Bud Break	$Y = 0.04X + 108.08$	0.001	0.52	Cogradient
2015	Initial Bud Break	$Y = -1.25X + 161.58$	0.09	< 0.01*	Countergradient
2016	Initial Bud Break	$Y = 0.80X + 80.20$	0.06	< 0.01*	Cogradient
2017	Initial Bud Break	$Y = 0.76X + 77.93$	0.06	< 0.01*	Cogradient
2013	Full Bud Break	$Y = 0.40X + 92.36$	0.12	< 0.01*	Cogradient
2014	Full Bud Break	$Y = -0.23X + 124.86$	0.04	< 0.01*	Countergradient
2015	Full Bud Break	$Y = -0.15X + 125.70$	0.002	0.41	Countergradient
2016	Full Bud Break	$Y = 0.87X + 80.84$	0.08	< 0.01*	Cogradient
2017	Full Bud Break	$Y = 0.24X + 99.71$	0.005	0.33	Cogradient
2013	Full Leaf Coloration	$Y = -2.63X + 372.90$	0.43	< 0.01*	Cogradient
2014	Full Leaf Coloration	$Y = -2.62X + 374.09$	0.45	< 0.01*	Cogradient
2015	Full Leaf Coloration	$Y = -2.60X + 372.12$	0.27	< 0.01*	Cogradient
2016	Full Leaf Coloration	$Y = -2.24X + 365.41$	0.25	< 0.01*	Cogradient
2013	Full Leaf Fall	$Y = -3.10X + 393.99$	0.47	< 0.01*	Cogradient
2014	Full Leaf Fall	$Y = -2.96X + 389.06$	0.48	< 0.01*	Cogradient
2015	Full Leaf Fall	$Y = -3.56X + 410.81$	0.35	< 0.01*	Cogradient
2016	Full Leaf Fall	$Y = -3.53X + 416.21$	0.37	< 0.01*	Cogradient

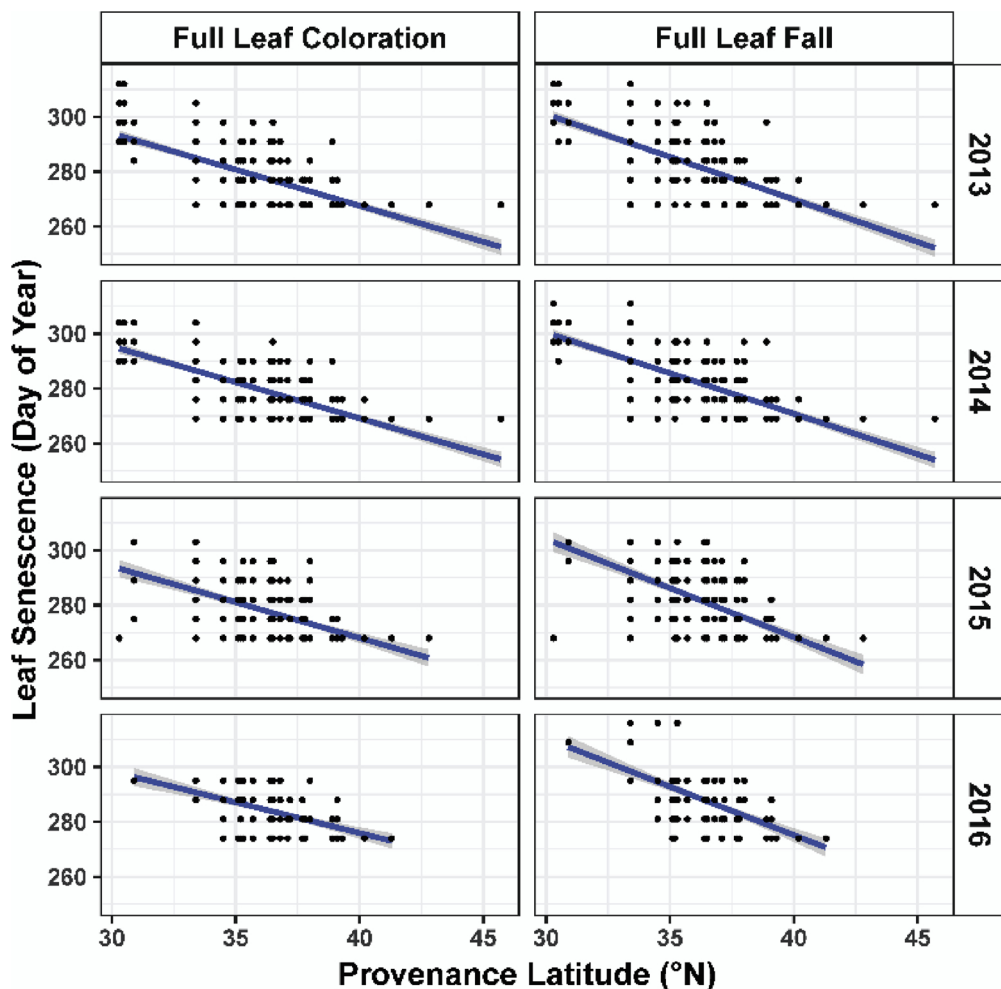


Fig. 5. Annual gradients of Full Leaf Coloration and Full Leaf Fall dates (in Day of Year) relative to provenance latitude (Cf. Table 2). All slopes of different years are negative and indicate a consistent cogradient pattern.

A close look at the spring phenology gradient (i.e., slope) values in comparison to seasonal mean temperatures revealed a coupled relationship with respect to their interannual variability (Fig. 6). The years showing significant countergradient patterns (2015 for IBB; and 2014 for FBB) were characterized with colder winter temperatures that

afforded greater chilling fulfillment opportunities. While years with significant cogradient patterns (2013, 2016, 2017 for IBB; 2013, 2016 for FBB) had relatively warmer temperatures in the prior winters (hence with lesser chilling fulfillment opportunities). The coldest winter and coolest spring in 2015 corresponded with the most pronounced

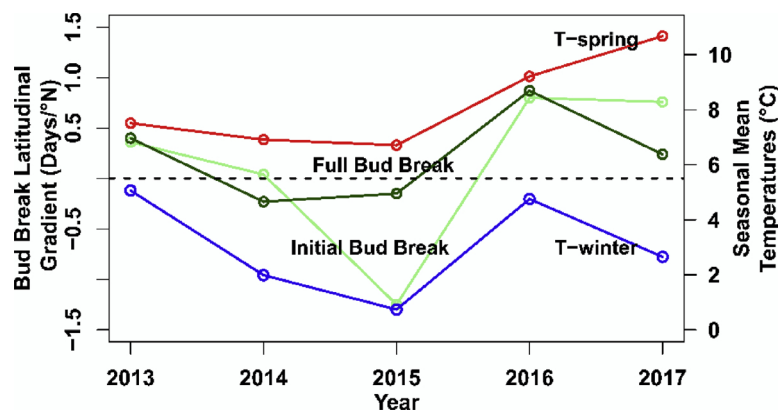


Fig. 6. Side-by-side comparison of the interannual variations of the latitudinal gradients of bud break dates (according to provenance locations) with the seasonal mean temperatures at the common garden.

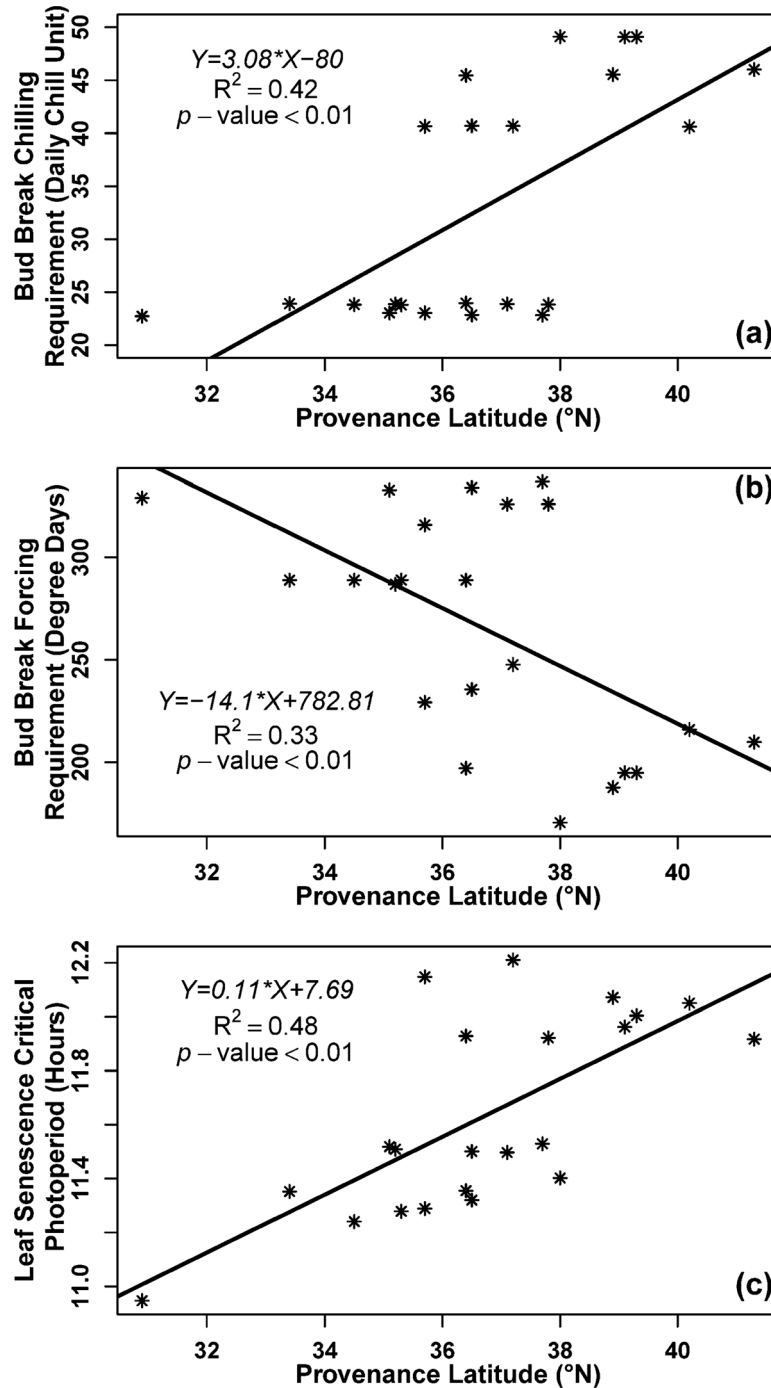


Fig. 7. Latitudinal gradients with linear equations of the critical environmental requirements of (a) chilling, (b) forcing, and (c) photoperiod as fitted for bud break and leaf senescence models with respect to different provenance locations.

countergradient pattern in IBB timing. Conversely, the strongest co-gradient pattern for both IBB and FBB occurred in the warm spring of 2016, following also a relatively warm winter.

3.3. Latitudinal gradients of environmental requirements

Critical parameter values fitted for provenance-specific models further revealed significant latitudinal gradients in environmental requirements of respective phenological development processes (Fig. 7, Table S1). Bud break models based on IBB dates showed gradually increasing chilling requirement (23~49 daily chill units) and gradually

decreasing forcing requirement (337~171 degree days) towards higher latitudes. The leaf senescence models built upon FLC dates showed increasing critical day length requirement (11–12 h) with latitude, but with no apparent geographic patterns found for other parameters.

3.4. Model testing and simulation with NPN data

The internally determined RMSE of provenance-specific spring models ranged from about 4.4 to 8.7 days, with a mean error of 6.7 days (Table 3). As noted previously, while the spring models were tested externally against the NPN observations, the fall models were

Table 3

Root mean square errors (*RMSE*, in days) for internal testing of spring and autumn models by provenance; and root mean square errors for prediction (*RMSEP*, in days) for external testing of autumn models only from leave-out-one cross-validation; *N* denotes the sample size.

Provenance	Spring models		Autumn models		
	RMSE	N	RMSE	RMSEP	N
4	4.7	37	3.5	3.5	30
5	4.6	22	4.3	4.4	19
6	5.5	31	4.6	5.0	26
7	6.2	75	5.6	5.8	60
8	5.2	44	7.2	7.2	37
9	4.4	41	8.2	9.1	34
10	7.6	155	4.6	4.6	121
11	7.4	51	5.3	6.1	40
12	5.8	77	6.0	7.1	61
13	8.1	87	6.9	7.3	68
14	6.4	197	7.2	7.2	155
15	7.7	103	8.4	9.3	81
16	7.2	80	7.7	8.8	64
17	7.9	51	5.2	5.3	41
18	5.5	73	6.3	6.8	58
19	6.7	69	5.7	5.8	56
20	7.6	64	6.8	7.2	51
21	7.4	51	7.0	7.1	42
22	8.3	63	6.5	7.3	50
23	7.0	95	6.9	7.1	77
24	8.3	94	10.2	10.2	77
25	8.7	27	6.4	7.0	23
Max	8.7		10.2	10.2	
Min	4.4		3.5	3.5	
Mean	6.7		6.4	6.8	

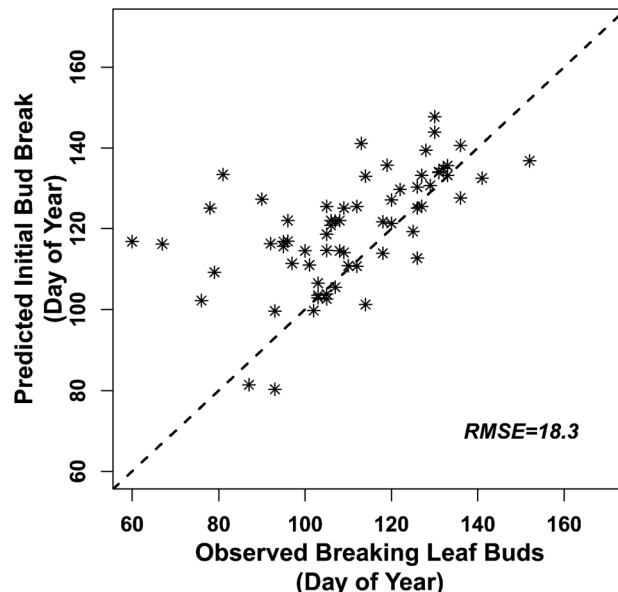


Fig. 8. Scatter plot of spatial model predictions of Initial Bud Break dates vs. National Phenology Network (NPN) observed Breaking Leaf Buds dates; with 1:1 line. The *RMSE* is in days.

additionally tested using *RMSEP* given a lack of corresponding NPN data. The *RMSE* and *RMSEP* (from leave-out-one cross-validation for external testing) of autumn models were similar, both ranging from 3.5 to 10.2 days, and with mean errors of 6.4 and 6.8 days, respectively. The external testing of spring model predictions against independent NPN observations at respective years/locations yielded an *RMSE* of 18.3 days between the predicted IBB and observed BLB dates (Fig. 8). The predicted IBB dates are biased towards being later than BLB observations.

The difference and similarity of spatial model (developed over the

common garden data) predictions and average model (based directly on the NPN data) predictions relative to NPN observations are further seen in the comparison of their latitudinal gradients (Fig. 9; Table 4). In both cases, the predicted gradients in terms of linear model intercept and slope did not differ from the observations significantly ($\alpha = 0.05$). This is based on the overlapped confidence intervals estimated from the bootstrapping analysis (Table 4). However, while spatial model predictions are consistently higher than observations (Cf. Fig. 8), the predicted slope is very close to that of observations (Fig. 9a, Table 4). On the other hand, predictions of the average model using NPN data is biased towards being earlier at lower latitudes and later at higher latitudes than observations (Fig. 9b). Despite that the difference is not statistically significant, the average model predictions are marked with a steeper slope than that of both the observations and the spatial model predictions.

4. Discussion

The spatially explicit modeling analysis underscored provenance-specific phenoclimatic requirements of white ash as a result of climatic adaptation. In general, the varied environmental requirements of spring and autumn phenology reflect adaptation to shortening growing seasons towards higher latitudes (Häminen, 2016). The latitudinal increase of chilling requirement of leaf bud break reflects adaptation to colder winter-spring temperatures, and the increased forcing requirement at lower latitudes shows adaptation to warmer spring temperatures. In addition, leaf senescence models highlighted the role of critical photoperiod, which increases with latitude, resulting from adaptation to longer day lengths at higher latitudes during the time period from summer solstice to autumnal equinox. These generalized relationships require further studies given that they underlie observed patterns which may be manifested in different ways and with varied characteristics for different species under diverse environmental conditions (Aitken and Hannerz, 2001; Alberto et al., 2013; Liang, 2016).

In particular, it is important to note that the observed gradients/clines of spring phenology may show opposite directions for the same species at different provenance trial locations (Kriebel, 1957; Kriebel and Wang, 1962), and as revealed in this study, even at the same common garden in different years. This is likely due to the interaction of chilling and forcing (Aitken and Hannerz, 2001), which are mutually constraining and difficult to disentangle. Each of the two elements, if allowed to operate alone, would lead to the manifestation of a distinct cogradient or countergradient from the same group of tree provenances. Liang (2016) discussed three factors that potentially affect the expression of alternative gradient patterns from common garden experiments: 1) general levels of chilling and forcing that are required by a species under study; 2) direction and magnitude of the temperature differences simulated by seed transfers from tree origin locations to the common garden; and 3) seasonal temperature regimes at a common garden in specific years. In the current study, northern/high-latitude provenances that demand higher chilling more likely have their dormancy release retarded by warmer climate at the common garden—favoring the expression of a cogradient pattern. On the other hand, as the common garden is located in the central range of the species, fulfillment of the higher forcing requirements of the southern provenances may be similarly compromised—contributing to the expression of a countergradient pattern. Hence, depending on the winter-spring weather conditions of a specific year, either scenario may stand out over the other. In many cases, however, the manifested spatial gradient may be weak or transitional as the two mechanisms cancel or balance each other out, as also shown in the current study. In addition, the latitudinal relationship may be overridden by additional climatic gradients, such as maritime-continental (i.e., longitudinal) and elevational gradients in different climatic regions (Robson et al., 2013; Von Wuehlisch et al., 1995).

Further, the comparison with NPN observations suggested that

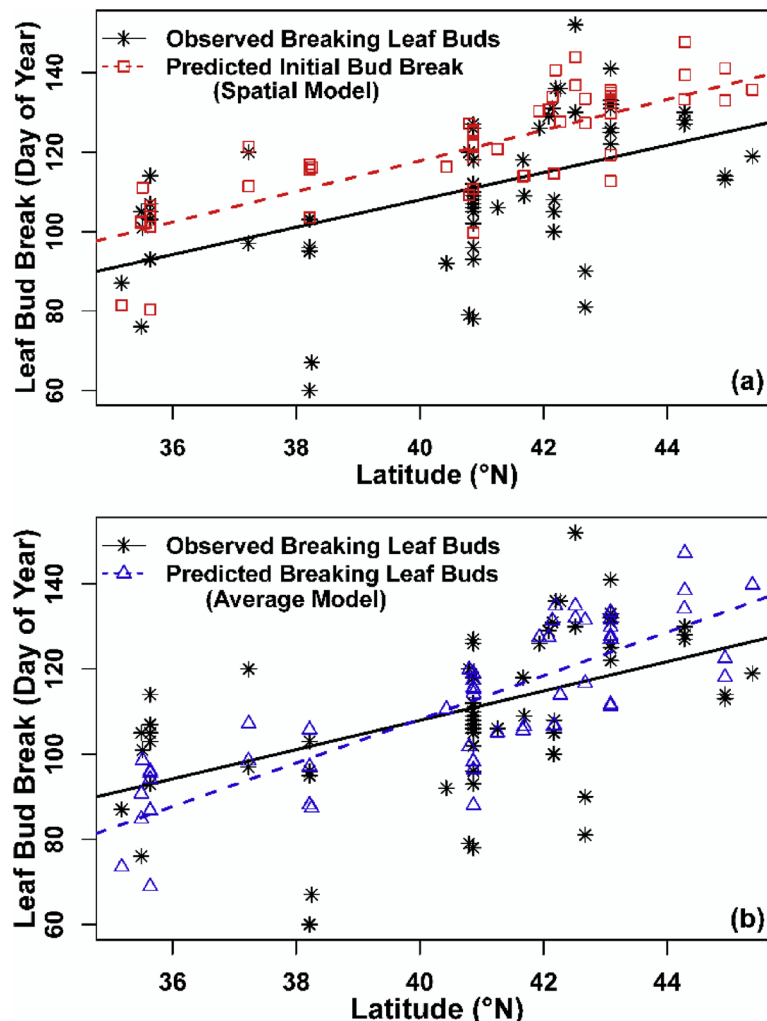


Fig. 9. Side-by-side comparison along latitude of (a) spatial model (based on parameters determined from common garden data) predicted Initial Bud Break dates and National Phenology Network (NPN)-observed Breaking Leaf Buds dates (in Day of Year), and (b) average model (fitted over all NPN data) predicted and NPN-observed Breaking Leaf Buds dates.

Table 4

Parameters of the leaf bud break linear models (Cf. Fig. 9) with confidence intervals ($\alpha = 0.05$) based on 10,000 times of bootstrapping (Davison and Hinkley, 1997). The linear models were fitted against latitude for National Phenology Network (NPN) observations, spatial model predictions, and average model predictions, respectively.

		Parameters		Confidence Interval ($\alpha = 0.05$)	
		Original	BootMean	Lower Limit	Upper Limit
NPN observations	Intercept	-29.74	-30.93	-85.71	15.94
	Slope	3.44	3.47	2.32	4.81
Spatial model predictions	Intercept	-36.51	-36.26	-69.31	-5.72
	Slope	3.86	3.85	3.10	4.65
Average model predictions	Intercept	-96.76	-97.73	-134.92	-63.65
	Slope	5.12	5.15	4.30	6.06

considering differential phenoclimatic requirements of plant populations may help reduce geographic biases in phenological predictions. Despite a systematic difference between predicted Initial Bud Break and observed Breaking Leaf Buds that may be potentially caused by observation/protocol difference and cross-site phenotypic plasticity of populations (Kramer et al., 2017), the spatial model that used genotype-specific parameter values predicted the observed latitudinal gradient more closely than the average model. The steeper slope of the average model predictions mimics that of cloned plant phenology, both without

considering genotypic difference among populations (Liang and Schwartz, 2014). Under the assumption that chilling fulfillment of naturally growing plants (vs. those in common gardens) is largely unhindered under the current climate at their original locations (but see Liang and Zhang, 2016), the observed temporal sequence of bud break across space would be mostly driven by their different forcing requirements. Hence, the steeper latitudinal gradient of average model predictions is likely caused by an overestimation of the forcing requirement of the populations at higher latitudes and at the same time

an underestimation for populations at lower latitudes. This is also the case when a cloned plant-based model is used to predict leaf-out phenology across a broad geographic area (Liang et al., 2016). In a climate change context, this adaptation-based latitudinal difference cannot be ignored because, for instance, the same magnitude of warming may lead to more advanced (earlier) spring phenology at northern locations (due to a lower forcing requirement) than that at southern locations (Jeong et al., 2013).

Autumn phenological patterns as revealed in this study highlighted the role of photoperiod in regulating the induction of growth cessation (Maurya and Bhalerao, 2017; Vaartaja, 1959; Way and Montgomery, 2014). The highly consistent cogradient pattern among white ash provenances across years concurs with a photoperiod-based latitudinal gradient of most if not all temperate tree species (Alberto et al., 2013; Fracheboud et al., 2009; Hall et al., 2007; Nienstaedt, 1974). A predominant photoperiod cue may help ensure timely leaf senescence and withdrawal of nutrients from leaves to stems prior to hard-to-predict first frosts (Gan and Amasino, 1997; Taiz and Zeiger, 2010), but temperature variation remains influential on interannual variability and long-term trends (Q. Liu et al., 2016; G. Liu et al., 2018; Rohde et al., 2011; Yang et al., 2015). As the research in autumn phenology moves forward, it is helpful to distinguish the *routine drivers* (i.e., photoperiod and temperature; Jeong and Medvighy, 2014; Maurya and Bhalerao, 2017) from the *stress factors* such as herbivore attacks, drought stresses, and other environmental changes that may lead to additional interannual variability (Panchen et al., 2015; Xie et al., 2015). In this study, a larger interannual variation of Full Leaf Fall dates compared to Full Leaf Coloration dates may indicate that the timing of the former phenophase, in relation to leaf abscission, is additionally affected by irregular wind incidents (as is also intuitively perceived in field observation). The emerald ash borer infestation could be another stress factor on some trees observed in this study, but more data would be needed to quantify it.

The modeling analysis employed in this study focused on delineation of provenance-specific climatic requirements of white ash for phenological development. Model selection and parameterization mostly followed common practices of previous work. Given the insufficient knowledge about the exact ecophysiological processes that occurred prior to the dates of phenological events, models developed in the study are unavoidably subject to a common pitfall of lacking realism (vs. accuracy; Hänninen, 2016). For instance, the choice of model types and *a priori* information based on studies of other species or determined empirically may not match the actual ecophysiology of white ash. In addition, fixed temperature responses were assumed for both spring and autumn phenology models, while different provenances may actually vary in their response mechanisms. More experimental studies that contribute directly to an ecophysiological understanding of the phenological processes of the species would be an ultimate solution to this problem. In the meantime, investigating additional species and developing better approaches to spatially-explicit phenological modeling will also be useful. Lastly, given that human modification of plant communities and natural gene flow among populations can complicate and homogenize plant genotypic differences over space (Chuine et al., 2000), widely distributed native species with more distinguishable geographic clines (Wright et al., 1958) should be focused on in the future.

5. Conclusions

Improved phenological forecasting requires accounting for geographic adaptation patterns of temperate trees in continental-scale phenological models. This study utilized observations from a white ash common garden to analyze and model genotype-specific variations of spring and autumn phenology. Results first showed that interannual variations in the common garden can help reveal the underlying climate adaptation patterns. The models fitted for specific tree provenances

further differentiated their different phenoclimatic requirements by latitude. A comparison with NPN observed bud break phenology suggested that omission of plant adaptation in models can potentially lead to geographically biased predictions towards northern and southern ranges of the species. Thus by considering genotypic variations based on specified adaptive patterns of plants, phenological forecasting may be done in a manner that is more spatially relevant and locally accurate. Certainly, such predictions cannot be tied to individual plants directly but would represent the spatial variability of phenoclimatic relationships of a given species within its native range. Given the importance of phenology as an indicator of biosphere-climate interactions, the ability to predict phenological timing in a spatially-explicit manner is useful for better forecasting of a broad range of related ecological processes.

Acknowledgments

I appreciate the help of Dr. Songlin Fei for accessing the common garden used in this study. Jeffrey F. Lewis with the USDA Forest Service, Daniel Boone National Forest, Morehead District provided valuable information about the plantation, maintained the plantation, and treated part of the plantation in response to the emerald ash borer infestation. UK geography graduate student Li-Chih Hsu facilitated data recording in spring 2016. I thank Dr. Jixiang Wu for providing valuable statistical analysis support. Dr. Heikki Hänninen reviewed this work and provided insightful and helpful comments. Dr. Darrell Napton kindly proofread the final version of the manuscript. I sincerely appreciate the help of these individuals along the way of completing this study. Part of the data was provided by the USA National Phenology Network and the many participants who contribute to its Nature's Notebook program. The study was partly supported by a start-up fund from the University of Kentucky. Finally, I thank the three reviewers for their constructive comments that greatly improved this work.

Appendix A. Supplementary data

Supplementary material related to this article can be found, in the online version, at doi:<https://doi.org/10.1016/j.agrformet.2018.12.004>.

References

- Aitken, S.N., Hannerz, M., 2001. Genecology and gene resource management strategies for conifer cold hardness. In: Biggs, S.J.C.F.J. (Ed.), Conifer Cold Hardiness. Springer, Dordrecht, Netherlands, pp. 23–53.
- Alberto, F.J., Aitken, S.N., Alfa, R., González-Martínez, S.C., Hänninen, H., Kremer, A., Lefèvre, F., Lenormand, T., Yeaman, S., Whetten, R., 2013. Potential for evolutionary responses to climate change—evidence from tree populations. *Glob. Change Biol.* 19 (6), 1645–1661.
- Aslaksen, H., 2010. The Mathematics of the Chinese Calendar. National University of Singapore (accessed 18 August 2018). <http://www.math.nus.edu.sg/aslaksen/calendar/chinese.shtml>.
- Ault, T.R., Zurita-Milla, R., Schwartz, M.D., 2015. A Matlab® toolbox for calculating spring indices from daily meteorological data. *Comput. Geosci.* 83, 46–53.
- Balzarolo, M., Vicca, S., Nguy-Robertson, A.L., Bonal, D., Elbers, J.A., Fu, Y.H., Grünwald, T., Horemans, J.A., Papale, D., Peñuelas, J., Suyker, A., Veroustraete, F., 2016. Matching the phenology of Net Ecosystem Exchange and vegetation indices estimated with MODIS and FLUXNET in-situ observations. *Remote Sens. Environ.* 174, 290–300.
- Basler, D., Körner, C., 2014. Photoperiod and temperature responses of bud swelling and bud burst in four temperate forest tree species. *Tree Physiol.* 34 (4), 377–388.
- Bey, C.F., Kung, F.H., Daniels, R.A., 1976. Genotypic variation in white ash—nursery results. *Proc. the Tenth Central States For. Tree Improv. Conf.* 141–145.
- Bonhomme, M., Rageau, R., Lacointe, A., 2010. Optimization of endodormancy release models, using series of endodormancy release data collected in France. *VIII International Symposium on Temperate Zone Fruits in the Tropics and Subtropics* 872, 51–60.
- Chuine, I., 2000. A unified model for budburst of trees. *J. Theor. Biol.* 207 (3), 337–347.
- Chuine, I., 2010. Why does phenology drive species distribution? *Philos. Trans. R. Soc. London, Ser. B* 365 (1555), 3149–3160.
- Chuine, I., Beaubien, E.G., 2001. Phenology is a major determinant of tree species range. *Ecol. Lett.* 4 (5), 500–510.
- Chuine, I., Régnière, J., 2017. Process-based models of phenology for plants and animals. *Annu. Rev. Ecol. Evol. Syst.* 48, 159–182.

- Chuine, I., Belmonte, J., Mignot, A., 2000. A modelling analysis of the genetic variation of phenology between tree populations. *J. Ecol.* 88 (4), 561–570.
- Chuine, I., Morin, X., Bugmann, H., 2010. Warming, photoperiods, and tree phenology. *Science* 329 (5989), 277–278.
- Chuine, I., Cortázar-Atauri, I.Gd., Kramer, K., Hänninen, H., 2013. Plant development models. In: Schwartz, M.D. (Ed.), *Phenology: An Integrative Environmental Science*. Springer, Dordrecht, pp. 275–294.
- Chuine, I., Bonhomme, M., Legave, J.M., García de Cortázar-Atauri, I., Charrier, G., Lacointe, A., Améglio, T., 2016. Can phenological models predict tree phenology accurately in the future? The unrevealed hurdle of endodormancy break. *Glob. Change Biol.* 22 (10), 3444–3460.
- Churkina, G., Schimel, D., Braswell, B.H., Xiao, X., 2005. Spatial analysis of growing season length control over net ecosystem exchange. *Glob. Change Biol.* 11 (10), 1777–1787.
- Clausen, K.E., 1980. Survival and early growth of diploid white ash planted in the central hardwood region. *Proc. Central Hardwood For. Conf.* III 374–383.
- Clausen, K.E., Kung, F.H., Bey, C.F., Daniels, R.A., 1981. Variation in white ash. *Silvae Genet.* 30 (2–3), 93–97.
- Cooke, J.E., Eriksson, M.E., Juntila, O., 2012. The dynamic nature of bud dormancy in trees: environmental control and molecular mechanisms. *Plant Cell Environ.* 35 (10), 1707–1728.
- Crimmins, T.M., Crimmins, M.A., Gerst, K.L., Rosemartin, A.H., Weltzin, J.F., 2017. USA National Phenology Network's volunteer-contributed observations yield predictive models of phenological transitions. *PLoS One* 12 (8), e0182919.
- Davison, A.C., Hinkley, D.V., 1997. *Bootstrap Methods and Their Application*. Cambridge University Press, Cambridge, UK and New York.
- Delpierre, N., Dufrêne, E., Soudani, K., Ulrich, E., Cecchini, S., Boé, J., François, C., 2009. Modelling interannual and spatial variability of leaf senescence for three deciduous tree species in France. *Agric. For. Meteorol.* 149 (6–7), 938–948.
- Donoso, I., Stefanescu, C., Martínez-Abrain, A., Traveset, A., 2016. Phenological asynchrony in plant–butterfly interactions associated with climate: a community-wide perspective. *Oikos* 1434–1444.
- Flint, H.L., 1974. Phenology and genecology of woody plants. In: Lieth, H. (Ed.), *Phenology and Seasonality Modeling*. Springer-Verlag, New York, pp. 83–97.
- Fogelström, E., Olofsson, M., Posledovich, D., Wiklund, C., Dahlgren, J.P., Ehrlén, J., 2017. Plant–herbivore synchrony and selection on plant flowering phenology. *Ecology* 98 (3), 703–711.
- Fracheboud, Y., Luquez, V., Björkén, L., Sjödin, A., Tuominen, H., Jansson, S., 2009. The control of autumn senescence in European aspen. *Plant Physiol.* 149 (4), 1982–1991.
- Gallatin, A.S., Primack, R.B., Wagner, D.L., 2015. Autumn, the neglected season in climate change research. *Trends Ecol. Evol.* 30 (3), 169–176.
- Gan, S., Amasino, R.M., 1997. Making sense of senescence (molecular genetic regulation and manipulation of leaf senescence). *Plant Physiol.* 113 (2), 313–319.
- Hall, D., Luquez, V., Garcia, V.M., St Onge, K.R., Jansson, S., Ingvarsson, P.K., 2007. Adaptive population differentiation in phenology across a latitudinal gradient in European aspen (*Populus tremula*, L.): a comparison of neutral markers, candidate genes and phenotypic traits. *Evol.* 61 (12), 2849–2860.
- Hänninen, H., 2016. *Boreal and Temperate Trees in a Changing Climate*. Dordrecht: Springer, Netherlands.
- Hänninen, H., Kramer, K., 2007. A framework for modelling the annual cycle of trees in boreal and temperate regions. *Silva Fenn.* 41 (1), 167–205.
- Hufkens, K., Basler, D., Milliman, T., Melaas, E.K., Richardson, A.D., 2018. An integrated phenology modelling framework in R. *Methods Ecol. Evol.* 9 (5), 1276–1285.
- Jeong, S.J., Medvigy, D., 2014. Macroscale prediction of autumn leaf coloration throughout the continental United States. *Global Ecol Biogeogr* 23 (11), 1245–1254.
- Jeong, S.J., Medvigy, D., Sheviakova, E., Malyshov, S., 2013. Predicting changes in temperate forest budburst using continental-scale observations and models. *Geophys. Res. Lett.* 40 (2), 359–364.
- Kramer, K., van der Werf, B., Schelhaas, M.J., 2015. Bring in the genes: genetic-ecophysiological modeling of the adaptive response of trees to environmental change with application to the annual cycle. *Front. Plant Sci.* 5, 742.
- Kramer, K., Ducousoo, A., Gömöry, D., Hansen, J.K., Ionita, L., Liesebach, M., Lorentz, A., Schüler, S., Sulkowska, M., de Vries, S., von Wühlisch, G., 2017. Chilling and forcing requirements for foliage bud burst of European beech (*Fagus sylvatica* L.) differ between provenances and are phenotypically plastic. *Agric. For. Meteorol.* 234–235, 172–181.
- Kriebel, H.B., 1957. Patterns of Genetic Variation in Sugar Maple. Ohio Agric. Exp. Station Res. Bull. 791, Wooster, Ohio.
- Kriebel, H.B., Wang, C.W., 1962. The interaction between provenance and degree of chilling in bud-break of sugar maple. *Silvae Genet.* 11 (5/6), 125–130.
- Lechowicz, M.J., 1984. Why do temperate deciduous trees leaf out at different times? Adaptation and ecology of forest communities. *Am. Nat.* 124 (6), 821–842.
- Liang, L., 2015. Geographic variations in spring and autumn phenology of white ash in a common garden. *Phys. Geogr.* 36 (6), 489–509.
- Liang, L., 2016. Beyond the Bioclimatic Law: geographic adaptation patterns of temperate plant phenology. *Prog. Phys. Geogr.* 40, 811–834.
- Liang, L., Schwartz, M.D., 2014. Testing a growth efficiency hypothesis with continental-scale phenological variations of common and cloned plants. *Int. J. Biometeorol.* 58 (8), 1789–1797.
- Liang, L., Schwartz, M.D., Fei, S., 2011. Validating satellite phenology through intensive ground observation and landscape scaling in a mixed seasonal forest. *Remote Sens. Environ.* 115, 143–157.
- Liang, L., Schwartz, M., Zhang, X., 2016. Mapping temperate vegetation climate adaptation variability using normalized land surface phenology. *Climate* 4 (2), 24.
- Liang, L., Zhang, X., 2016. Coupled spatiotemporal variability of temperature and spring phenology in the Eastern United States. *Int. J. Climatol.* 36 (4), 1744–1754.
- Lieth, H., 1974. Phenology and Seasonal Modeling. *Ecological Studies, Analysis and Synthesis*, 8. Springer-Verlag, New York.
- Little Jr, E.L., 1971. *Atlas of United States trees. Conifers and Important Hardwoods*. Miscellaneous Publication 1146 Vol. 1 U.S. Department of Agriculture, Forest Service, Washington, DC.
- Liu, Q., Fu, Y.H., Zhu, Z., Liu, Y., Liu, Z., Huang, M., Janssens, I.A., Piao, S., 2016. Delayed autumn phenology in the Northern Hemisphere is related to change in both climate and spring phenology. *Glob. Change Biol.* 22 (11), 3702–3711.
- Liu, G., Chen, X., Zhang, Q., Lang, W., Delpierre, N., 2018. Antagonistic effects of growing season and autumn temperatures on the timing of leaf coloration in winter deciduous trees. *Glob. Change Biol.* 24 (8), 3537–3545.
- Marchin, R., 2006. Population Variation in *Fraxinus americana* L. (white ash) in a Common Garden at the Edge of the Species Range. University of Kansas, Lawrence, KS MA Thesis.
- Mátyás, C., 1996. Climatic adaptation of trees: rediscovering provenance tests. *Euphytica* 92 (1), 45–54.
- Maurya, J.P., Bhalerao, R.P., 2017. Photoperiod- and temperature-mediated control of growth cessation and dormancy in trees: a molecular perspective. *Ann. Bot.* 120 (3), 351–360.
- Melaas, E.K., Richardson, A.D., Friedl, M.A., Dragoni, D., Gough, C.M., Herbst, M., Montagnani, L., Moors, E., 2013. Using FLUXNET data to improve models of springtime vegetation activity onset in forest ecosystems. *Agric. For. Meteorol.* 171–172, 46–56.
- Morin, X., Thuiller, W., 2009. Comparing niche-and process-based models to reduce prediction uncertainty in species range shifts under climate change. *Ecology* 90 (5), 1301–1313.
- Nienstaedt, H., 1974. Genetic variation in some phenological characteristics of forest trees. In: Lieth, H. (Ed.), *Phenology and Seasonality Modeling*. Springer-Verlag, New York, pp. 389–400.
- Panchen, Z.A., Primack, R.B., Gallatin, A.S., Nordt, B., Stevens, A.D., Du, Y., Fahey, R., 2015. Substantial variation in leaf senescence times among 1360 temperate woody plant species: implications for phenology and ecosystem processes. *Ann. Bot.* 116, 865–873.
- Preite, V., Stöcklin, J., Armbruster, G.F.J., Scheepens, J.F., 2015. Adaptation of flowering phenology and fitness-related traits across environmental gradients in the widespread *Campanula rotundifolia*. *Evol. Ecol.* 29 (2), 249–267.
- R Core Team, 2018. *R: A Language and Environment for Statistical Computing*. R Foundation for Statistical Computing, Vienna, Austria.
- Rafferty, N.E., CaraDonna, P.J., Bronstein, J.L., 2015. Phenological shifts and the fate of mutualisms. *Oikos* 124 (1), 14–21.
- Richardson, E., Seeley, S., Walker, D., 1974. A model for estimating the completion of rest for Red hawthorn and Elbert peach tree. *HortScience* 9, 331–332.
- Richardson, A.D., Bailey, A.S., Denny, E.G., Martin, C.W., O'keefe, J., 2006. Phenology of a northern hardwood forest canopy. *Glob. Change Biol.* 12 (7), 1174–1188.
- Richardson, A.D., Andy Black, T., Cais, P., Delbart, N., Friedl, M.A., Gobron, N., Hollinger, D.Y., Kutsch, W.L., Longdoz, B., Luyssaert, S., 2010. Influence of spring and autumn phenological transitions on forest ecosystem productivity. *Philos. Trans. Biol. Sci. 365 (1555)*, 3227–3246.
- Robson, T.M., Rasztovits, E., Aphalo, P.J., Alia, R., Aranda, I., 2013. Flushing phenology and fitness of European beech (*Fagus sylvatica* L.) provenances from a trial in La Rioja, Spain, segregate according to their climate of origin. *Agr. For. Meteorol.* 180 (0), 76–85.
- Rohde, A., Bhalerao, R.P., 2007. Plant dormancy in the perennial context. *Trends Plant Sci.* 12 (5), 217–223.
- Rohde, A., Bastien, C., Boerjan, W., 2011. Temperature signals contribute to the timing of photoperiodic growth cessation and bud set in poplar. *Tree Physiol.* 31 (5), 472–482.
- Schwartz, M.D., Ahas, R., Aasa, A., 2006. Onset of spring starting earlier across the Northern Hemisphere. *Glob. Change Biol.* 12 (2), 343–351.
- Schwartz, M.D., Ault, T.R., Betancourt, J.L., 2013. Spring onset variations and trends in the continental United States: past and regional assessment using temperature-based indices. *Int. J. Climatol.* 33 (13), 2917–2922.
- Taiz, L., Zeiger, E., 2010. *Plant Physiology*. Sinauer Associates, Sunderland, MA.
- USA National Phenology Network, 2017. *Plant and Animal Phenology Data*. Data type: Individual Phenometrics. 01/01/2011–12/31/2016 for Region: 50°, -60° (UR); 24°, -100° (LL). Data set accessed 06/14/2017 at <http://doi.org/10.5066/F78S4N1>.
- Vaartaja, O., 1959. Evidence of photoperiodic ecotypes in trees. *Ecol. Monogr.* 29 (2), 91–111.
- Vitasse, Y., Delzon, S., Bresson, C.C., Michalet, R., Kremer, A., 2009. Altitudinal differentiation in growth and phenology among populations of temperate-zone tree species growing in a common garden. *Can. J. For. Res.* 39 (7), 1259–1269.
- Von Wuehlisch, G., Krusche, D., Muhs, H., 1995. Variation in temperature sum requirement for flushing of beech provenances. *Silvae Genet.* 44, 343–345.
- Way, D.A., 2011. Tree phenology responses to warming: spring forward, fall back? *Tree Physiol.* 31 (5), 469–471.
- Way, D.A., Montgomery, R.A., 2014. Photoperiod constraints on tree phenology, performance and migration in a warming world. *Plant Cell Environ.* 38 (9), 1725–1736.
- Webb, D.P., 1976. Effects of cold storage duration on bud dormancy and root regeneration of white ash (*Fraxinus americana* L.) seedlings. *Hortscience* 11 (2), 155–157.
- Webb, D.P., 1977. Root regeneration and bud dormancy of sugar maple, silver maple, and white ash seedlings: effects of chilling. *Forest Sci.* 23 (4), 474–483.
- Wendel, G., 1984. Performance of White Ash Progenies After 7 Years in a West Virginia Planting. Proc. Northeastern Forest Tree Improvement Conf. (USA), Morgantown, WV.
- Wright, J.W., 1944. Genotypic variation in white ash. *J. For.* 42 (7), 489–495.
- Wright, J.W., 1976. *Introduction to Forest Genetics*. Academic Press, New York.
- Wright, J.W., Bingham, R., Dorman, K., 1958. Genetic variation within geographic

- ecotypes of forest trees and its role in tree improvement. *J. For.* 56 (11), 803–808.
- Wu, C., Gough, C.M., Chen, J.M., Gonsamo, A., 2013. Evidence of autumn phenology control on annual net ecosystem productivity in two temperate deciduous forests. *Ecol. Eng.* 60, 88–95.
- Xia, J., Niu, S., Ciais, P., Janssens, I.A., Chen, J., Ammann, C., Arain, A., Blanken, P.D., Cescatti, A., Bonal, D., Buchmann, N., Curtis, P.S., Chen, S., Dong, J., Flanagan, L.B., Frankenberg, C., Georgiadis, T., Gough, C.M., Hui, D., Kiely, G., Li, J., Lund, M., Magliulo, V., Marcolla, B., Merbold, L., Montagnani, L., Moors, E.J., Olesen, J.E., Piao, S., Raschi, A., Rouspard, O., Suyker, A.E., Urbaniak, M., Vaccari, F.P., Varlagin, A., Vesala, T., Wilkinson, M., Weng, E., Wohlfahrt, G., Yan, L., Luo, Y., 2015. Joint control of terrestrial gross primary productivity by plant phenology and physiology. *PNAS* 112 (9), 2788–2793.
- Xie, Y., Wang, X., Silander, J.A., 2015. Deciduous forest responses to temperature, precipitation, and drought imply complex climate change impacts. *PNAS* 112 (44), 13585–13590.
- Yang, Y., Guan, H., Shen, M., Liang, W., Jiang, L., 2015. Changes in autumn vegetation dormancy onset date and the climate controls across temperate ecosystems in China from 1982 to 2010. *Glob. Change Biol.* 21 (2), 652–665.
- Yu, R., Schwartz, M.D., Donnelly, A., Liang, L., 2016. An observation-based progression modeling approach to spring and autumn deciduous tree phenology. *Int. J. Biometeorol.* 60 (3), 335–349.
- Zohner, C.M., Renner, S.S., 2014. Common garden comparison of the leaf-out phenology of woody species from different native climates, combined with herbarium records, forecasts long-term change. *Ecol. Lett.* 17 (8), 1016–1025.